Suboptimal Kalman Filters for Target Tracking with Navigation Uncertainty in One Dimension

Edmund F. Brekke
Department of Engineering Cybernetics
NTNU
7034 Trondheim, Norway
edmund.brekke@itk.ntnu.no

Erik F. Wilthil
Department of Engineering Cybernetics
NTNU
7034 Trondheim, Norway
erik.wilthil@itk.ntnu.no

Abstract— **The vast majority of literature on target tracking assumes that the position and orientation of the tracking sensor is stationary and/or known. However, for many applications the sensor is mounted on a moving vehicle, whose motion only can be estimated with a non-negligible uncertainty. In this paper, we suggest seven possible architectures for Kalman filtering in the simplest such scenario that we can construct: Assuming that both the ownship and a single target moves along a straight line according to linear kinematics. Some of the tracking filters are parameterized in the stationary world frame, while others are parameterized the body frame of the ownship. Also, some of the tracking filters take correlations between target state and ownship state into account, while others neglect such correlations. Simulations demonstrate that the suboptimal architectures may or may not reach similar performance as the optimal filter, depending on the process noise of the target and the performance measure chosen. Simulations of multi-target scenarios demonstrate that compensation of navigation uncertainty generally can reduce track-loss rates and OSPA distance.**

TABLE OF CONTENTS

1. INTRODUCTION

In target tracking, the focus has traditionally been on moving targets (e.g., ships) tracked by means of a sensor (e.g., surveillance radar) whose position and orientation is fixed and known. However, many applications (e.g., collision avoidance for autonomous surface vehicles or driverless cars) lead to tracking problems where the sensor is mounted on a moving vehicle, known as the ownship. The tracking method must then take the motion of the ownship into account. Furthermore, errors in the ownship navigation will affect the errors of the tracking method.

Ownship navigation is typically carried out by means of an indirect, also known as error-state Kalman filter [1, 2] which performs fusion of measurements from sensors such as inertial measurement unit (IMU), compass and a global navigation satellite system (e.g., GPS). More accurate navigation can sometimes be achieved by estimating the position relative to known landmarks or transponders, or by means of simultaneous localization and mapping (SLAM), which also involves estimating a map of observed landmarks and keeping track of correlations between the landmarks and the ownship. Target tracking is typically carried out by means of a direct, also known as full-state, Kalman filter, which estimates position and velocity of a target by means of range and bearing measurements from an imaging sensor (e.g., radar). Target tracking can typically be decomposed in the two tasks of filtering and data association. In this paper, we are mainly concerned with the former task.

The optimal solution to the filtering part of target tracking with navigation uncertainty is found by generalizing SLAM to deal with moving landmarks. This entails maintaining a joint state vector of ownship state and target states with a corresponding joint covariance matrix. This may, however, be undesirable for several reasons. Allowing target measurements to affect the ownship navigation can be potentially disastrous if data association or filtering models faulty.

An alternative is to maintain correlations without allowing the target measurements to affect the ownship state. This is done in a Schmidt-Kalman filter (SKF). We may also opt for an even simpler solution: We can let the uncertainty of the ownship affect the target estimate, without maintaining any joint correlations. In addition to these issues, one may choose between representing the target state in the stationary world frame, in a body frame moving along with the ownship, or in some kind of hybrid frame.

This leads to several possible approaches to target tracking with navigation uncertainty. In [3], we studied three such filtering architectures for filtering with navigation in six degrees of freedom. In this paper we provide a more systematic comparison of several more filtering architectures, and we also study how the different architectures impact data association. We address the simplest possible scenario of relevance: A single target and the ownship are both moving in one dimension according to Gaussian-linear models.

The paper is organized as follows: In Section 2 we discuss previous work on the problem of target tracking with navigation uncertainty. In Section 3 we describe the estimation problem. We propose seven fundamental filtering architectures in Section 4. Simulation results for the filtering methods are discussed in Section 5. Results for multi-target scenarios with data association uncertainty are reported in Section 6. A conclusion follows in Section 7.

978-1-5090-1613-6/17/31.00

2. PREVIOUS WORK

As argued in Section 1, target tracking under navigation uncertainty is intimately linked to SLAM, and several researchers working on SLAM have dealt with moving targets as part of their SLAM methods. In [4], a generalized version of the PHD filter was used to solve the combined problem of SLAM and target tracking. A more general, but also more abstract, solution to the same problem was proposed in [5]. The simpler problem of detecting and tracking a single target using a moving platform was treated in [6]. All of these approaches were founded upon finite set statistics (FISST), and were implemented by means of Rao-Blackwellized particle filtering. Both [4] and [6] addressed the differences between SLAM and target tracking. In [4], separate maps were constructed for static SLAM features and for dynamic targets. In [6], the target measurements were prevented from affecting the ownship state in a manner similar to the SKF.

An EKF-based solution to the combination of SLAM and target tracking was outlined in [7]. The author of [7] recommended that targets should be tracked in the local body frame of the ownship, and that uncertainty pertaining to the ownship plant model should be injected into the resulting body frame process model of the target.

Another body of relevant research comes from sensor bias estimation using targets of opportunity [8]. Instead of estimating the bias, the authors of [9] proposed to treat the bias as a zero-mean nuisance parameter with known *a priori* statistics. The impact of the bias could then be mitigated by means of an SKF. The SKF was applied to the more general case of target tracking with navigation uncertainty in [10]. The authors of [10] parameterized the target state in the world frame, and argued that navigation uncertainty primarily is of importance when there is a need to transfer the tracking results to other applications in a global reference frame.

3. CONCEPTUAL FRAMEWORK

The moving platform tracking problem involves the following four models: Process model for the ownship state, process model for the target state, measurement model(s) for the ownship state and measurement model(s) for the target state.

Ownship process model

The ownship has the state vector $\eta = [\rho^\circ, v^\circ, b^\circ]^\mathsf{T}$, containing position ρ°, velocity v° and acelerometer bias b° of the ownship. In continuous time, the ownship state vector obeys the linear model $\dot{\eta} = F^\circ\eta + Bu + G^\circ n^\circ$ where

$$F^\circ = \begin{bmatrix} 0 & 1 & 0 \\ 0 & 0 & 1 \\ 0 & 0 & -\alpha \end{bmatrix}, \quad B = \begin{bmatrix} 0 \\ 1 \\ 0 \end{bmatrix}, \quad G^\circ = \begin{bmatrix} 0 & 0 \\ 1 & 0 \\ 0 & 1 \end{bmatrix}.$$

The input u is equal to the ownship acceleration. In the error-state *implementation* of the ownship navigation filter, the *measured* acceleration is used as input u, and the corresponding measurement noise is accounted for by the process noise n° in the filter. We model n° as a continuous-time white noise process distributed according to $\mathcal{N}(0, D^\circ\delta(t-\tau))$. The process noise covariance matrix is $D^\circ = \mathrm{diag}(\sigma_\mathrm{a}^2, \sigma_\mathrm{b}^2)$ where σ_a^2 is a continuous-time equivalent of the accelerometer noise covariance, while σ_b^2 is the covariance of driving noise of Gauss-Markov process of the accelerometer bias.

The continuous-time models are discretized exactly using Van Loan's method [11], yielding a model of the form

$$\eta_k = \Psi\eta_{k-1} + u_k + n_k^\circ$$

The discrete-time plant noise n_k° is a white sequence with covariance Q°, which also is given by the formulas in [11].

Target process model

Although the target kinematics can be speficied in any known reference frame, it is most natural to do this in an inertial frame, i.e., the world frame. We let the world frame state vector of the target be $x^w = [\rho^w, v^w]^\mathsf{T}$ where ρ^w is position and v^w is velocity in the world frame. The continuous time model is $\dot{x}^w = Fx^w + Gn$ where $n \sim \mathcal{N}(0, Q\delta(t-\tau))$ and where

$$F = \begin{bmatrix} 0 & 1 \\ 0 & 0 \end{bmatrix}, \quad Q = \sigma_v^2.$$

This is discretized to a discrete-time model of the form

$$x_k^w = \Phi x_{k-1}^w + n_k \tag{1}$$

where n_k is a zero-mean Gaussian white sequence whose covariance Q is given by the formulas in [11].

For future reference we also introduce the *ingenuous* body frame target vector x^b and the *factitious* body frame target vector x^f which are related to x^w according to

$$x^b = \begin{bmatrix} \rho^b \\ v^b \end{bmatrix} = x^w - E\eta, \quad E = \begin{bmatrix} 1 & 0 & 0 \\ 0 & 1 & 0 \end{bmatrix}$$
$$x^f = \begin{bmatrix} \rho^b \\ v^w \end{bmatrix} = x^w - T\eta, \quad T = \begin{bmatrix} 1 & 0 & 0 \\ 0 & 0 & 0 \end{bmatrix}.$$

Ownship measurement model

The navigation filter utilizes measurements of acceleration and world-frame position of the ownship. The acceleration measurements are used in the discrete-time inputs u_k of the navigation filter, so only the position measurements require a bona-fide measurement model. This model is

$$y_k = H^\circ\eta_k + m_k^\circ = H_{\xi y}[x_k^\mathsf{T}, \eta_k^\mathsf{T}]^\mathsf{T} + m_k^\circ \tag{2}$$

where $H^\circ = [1, 0, 0]$. We have also introduced the SLAM-like measurement matrix $H_{\xi y} = [0, 0, 1, 0, 0]$ for future reference. The noise sequence m_k° is zero-mean Gaussian white with covariance R°.

Target measurement model

We measure the body-frame position of the target (e.g., with a radar), and the measurement model can be written in the following three equivalent forms

$$\begin{aligned} z_k &= H(x_k^w - E\eta_k) + m_k = H(x_k^w - T\eta_k) + m_k \\ &= Hx_k^w - H^\circ\eta_k + m_k \end{aligned} \tag{3}$$

where $H = [1, 0]$ and where m_k is a zero-mean Gaussian white sequence with covariance R. Notice that z_k is used for target measurements while y_k is used for ownship measurements.

4. SEVEN ARCHITECTURES FOR TARGET TRACKING WITH NAVIGATION UNCERTAINTY

In this section we describe seven possible architectures for target tracking in the presence of navigation uncertainty. All the filters involve the following steps

1. Propagation (prediction) of ownship and target motion.
2. Ownship update, and possibly reframing of the target.
3. Target update.

By ownship update we mean the processing of a measurement of the model (2), while a target update means the processing of a measurement of the model (3).

The basic world-frame filter

The most straightforward way of performing target tracking on a moving platform is simply to use the state estimates of the ownship navigation in the measurement equation (3), while ignoring the corresponding navigation uncertainty. We call the resulting filter "World basic".

The SLAM-like approach

The optimal solution to the estimation problem described in Section 3 involves propagating the joint state vector $\xi_k = [\eta_k^\mathsf{T}, (x_k^w)^\mathsf{T}]^\mathsf{T}$ together with its covariance. Notice that we have chosen to to parameterize the target state in the world frame. We could also have developed the SLAM-like filter in the body frame, and that filter would also be optimal, and entirely equivalent to the world frame SLAM-like filter, despite the different implementation.

The propagation model—Let us introduce the SLAM-like transition matrix and the corresponding process noise covariance matrix given by

$$\Phi_\xi = \begin{bmatrix} \Phi & 0 \\ 0 & \Psi \end{bmatrix} \text{ and } Q_\xi = \begin{bmatrix} Q & 0 \\ 0 & Q^\circ \end{bmatrix}.$$

The propagation step is then given by

$$p(\xi_{k+1} \,|\, z^k, y^k) = \int \mathcal{N}(\xi_{k+1}\,;\, \Phi_\xi \xi_k, Q_\xi)\, p(\xi_k \,|\, z^k, y^k) \mathrm{d}\xi_k$$

which is solved by a standard Kalman filter propagation step insofar as the prior $p(\xi_k \,|\, z^k, y^k)$ is Gaussian, which is the case.

The ownship update—This step is a Kalman filter update for the likelihood $p(y_k \,|\, \xi_k) = \mathcal{N}(y_k\,;\, H_{\xi y}\xi_k, R^\circ)$ with prior expectation and covariance from the previous step.

The target update—Similarly, this step is a Kalman filter update for the likelihood $p(z_k \,|\, \xi_k) = \mathcal{N}(z_k\,;\, [H, -H^\circ]\xi_k, R)$ with prior expectation and covariance from the previous step.

The Schmidt-Kalman filter in world frame

The world frame SKF is quite similar to the SLAM-like filter, but with one important difference. During the target measurement update, the lower block in the joint Kalman gain is set to zero, thereby eliminating any flow of information into the ownship state. This ensures that information from the target measurements z_k never can enter the ownship state or its covariance. All the formulas required for implementation are straightforward to adapt from [9], with exception of equation (8) in that paper: Since the navigation state in our paper is time-varying with transition matrix Ψ, we must postmultiply with Ψ^T in the propagation of the cross-covariance.

The Schmidt-Kalman filter in body frame

The body frame SKF maintains a joint state vector which is different from the state vector of the previous two filters. Its state vector is $\xi_k^b = \left[(x_k^b)^\mathsf{T}, \eta_k^\mathsf{T}\right]^\mathsf{T}$. The corresponding covariance matrix is denoted

$$S_k^b = \begin{bmatrix} P_k^b & C_k \\ C_k^\mathsf{T} & P_k^\circ \end{bmatrix}.$$

where P_k° by the construction of the SKF is always identical to the covariance of the standalone ownship navigation, and P_k^b is the covariance of the body-parameterized target state as calculated by the body frame SKF.

The propagation step—Due to the parameterization in body frame, the propagation of the target state now depends on the propagation of the ownship state, leading to slightly different equations than those in [9]. The prediction is identical to what one would obtain for a body frame SLAM-like filter. It can be shown that the joint transition matrix is

$$\Phi_{\mathrm{SB}} = \begin{bmatrix} \Phi & \Phi E - E\Psi \\ 0 & \Psi \end{bmatrix}$$

while the joint process noise covariance matrix is

$$Q_{\mathrm{SB}} = \begin{bmatrix} Q + EQ^\circ E^\mathsf{T} & -EQ^\circ \\ -Q^\circ E^\mathsf{T} & Q^\circ \end{bmatrix}.$$

The prediction is then given by

$$\bar{\xi}_{k+1}^b = \Phi_{\mathrm{SB}}\, \hat{\xi}_k^b + \begin{bmatrix} -E \\ I \end{bmatrix} u_{k+1}$$
$$\bar{S}_{k+1}^b = \Phi_{\mathrm{SB}}\, \hat{S}_{k+1}^b\, \Phi_{\mathrm{SB}}^\mathsf{T} + Q_{\mathrm{SB}}$$

where the hat denotes previous estimate and the bar denotes current prediction. Proving these equations is straightforward by applying a linear transformation to the world frame SLAM-like state vector and utilizing standard results for multivariate Gaussians.

The ownship update and reframing—As for the world-frame SKF, receiving an ownship measurement y_k affects both ownship estimate and target estimate in the same manner as for the optimal SLAM-like filter. For brevity, the details are omitted.

The target update—Let $\bar{x}_k^b$ be the predicted state estimate of the target at time step k, let $\bar{P}_k^b$ be the corresponding covariance, and let $\bar{C}_k$ be the predicted cross-covariance with the ownship state. By setting the ownship part of the joint Kalman gain equal to zero, we are left with the target part of the Kalman gain, which is

$$W_k = \bar{P}_k^b H^\mathsf{T} (H \bar{P}_k^b H^\mathsf{T} + R)^{-1}.$$

The updated target state estimate, its covariance and its cross-covariance with the ownship state are then found as

$$\hat{x}_k^b = \bar{x}_k^b + W_k(z_k - H\bar{x}_k^b)$$
$$\hat{P}_k^b = (I - W_k H)\bar{P}_k^b$$
$$\hat{C}_k = \bar{C}_k - W_k H \bar{C}_k.$$

The updated joint state is then constructed by concatenating $\hat{x}_k^b$ with the standalone ownship prediction, and the same is done for the covariance.

The correlation-free world filter

The remaining three filters differ from the previous filters in that they compensate for navigation uncertainty without maintaining any cross-correlations between their target state vectors and the ownship state. For the correlation-free world filter, the target state vector is $x_k^w = [\rho_k^w, v_k^w]^\mathsf{T}$, and the corresponding covariance matrix maintained by the filter is denoted P_k^w.

The propagation step—The propagation step is trivial for this filter, as both target and ownship propagation are carried out independently according to $p(x_{k+1}^w \,|\, x_k^w)$ and $p(\eta_{k+1} \,|\, \eta_k)$ as specified in Section 3.

The ownship update and absence of reframing—Since this filter does not maintain target-ownship-correlations, it effectively treats the target as stochastically independent of the ownship. If Bayes rule is applied to the joint density under this assumption, it is easily seen that the target density is unaffected by any ownship measurement y_k. Therefore, the correlation-free world filter does not do any reframing of the target estimate when ownship measurements are received.

The target update—Recall that target measurements are received according to $z_k = Hx_k^w - G\eta_k + m_k$. Thus, despite *a priori* independence, the link between x_k^w and z_k is affected by the uncertainty in our estimate of η_k, and this should be taken into account in the measurement update.

PROPOSITION 1: Let the prior joint density of world frame target state and ownship state before observing z_k be

$$p(x_k^w, \eta_k \,|\, z^{k-1}) = \mathcal{N}\left(\begin{bmatrix} x_k^w \\ \eta_k \end{bmatrix}; \begin{bmatrix} \bar{x}_k^w \\ \bar{\eta}_k \end{bmatrix}, \begin{bmatrix} P_k^w & 0 \\ 0 & P_k^\circ \end{bmatrix}\right)$$

The marginal density of the world frame target state after observing z_k is then given by

$$p(x_k^w \,|\, z^k) = \mathcal{N}(x_k^w \,;\, \hat{x}_k^w, \hat{P}_k^w)$$

where

$$\begin{aligned}
\hat{x}_k^w &= \bar{x}_k^w + W(z_k - H\bar{x}_k^w - G\bar{\eta}) \\
\hat{P}_k^w &= P_k^w - P_k^w H^\mathsf{T}(HP_k^w H^\mathsf{T} + GP_k^\circ G^\mathsf{T} + R)^{-1} HP_k^w \\
W_k &= P_k^w H^\mathsf{T}(HP_k^w H^\mathsf{T} + GP_k^\circ G^\mathsf{T} + R)^{-1}.
\end{aligned}$$

Proof: This is seen by employing the fundamental product identity [12] on the product of Gaussians $p(z_k \,|\, x_k^w, \eta_k)\, p(x_k^w, \eta_k \,|\, z^{k-1})$ and marginalizing. ■

The ingenuous body filter

In the last two filters that we discuss, which we call the *ingenuous* and the *factitious* body filters, the position of the target is parameterized in the body frame of the ownship. In the ingenuous body filter, not only the target position, but also the target velocity is parameterized in the body frame. The state vector is $x_k^b = \left[\rho_k^b, v_k^b\right]^\mathsf{T}$. We call this filter ingenuous because it only tries to estimate how the target moves relative to the observer, and not how it moves relative to any other frame. For this filter, the disregard of correlations between the target and ownship amounts to assuming that x_k^b and η_k are *a priori* independent before any step in the filtering cycle.

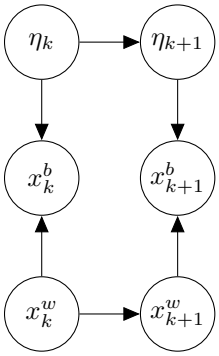

Figure 1: Dependencies in the ingenuous body filter.

The propagation step—In the propagation step, the objective of the filter is to evaluate the predicted density

$$p(x_{k+1}^b \,|\, z^k, y^k) = \int p(x_{k+1}^b \,|\, x_k^b) p(x_k^b \,|\, z^k, y^k)\, \mathrm{d}x_k^b.$$

Notice that the body-frame transition density $p(x_{k+1}^b \,|\, x_k^b)$ is *not* the same as the world frame target Markov model (1). In contrast, this density is given by marginalization of the joint density $p(x_{k+1}^b, x_{k+1}^w, x_k^w, \eta_{k+1}, \eta_k \,|\, x_k^b)$ over x_{k+1}^w, x_k^w, η_{k+1} and η_k. Nevertheless, we can find a Gaussian expression for $p(x_k^b \,|\, x_{k-1}^b)$, and thus obtain the predicted density $p(x_k^b \,|\, z^{k-1}, y^{k-1})$ by means of a standard Kalman filter prediction step.

PROPOSITION 2: The body-frame transition density is given by $p(x_{k+1}^b \,|\, x_k^b) = \mathcal{N}(x_{k+1}^b \,;\, a_{k+1}^b,\, Q_{k+1}^b)$ where

$$\begin{aligned}
a_{k+1}^b &= \Phi x_k^b + (\Phi E - E\Psi)\, \hat{\eta}_k + Eu_{k+1} \\
Q_{k+1}^b &= Q + EQ^\circ E^\mathsf{T} + (\Phi E - E\Psi)\, P_k^\circ\, (\Phi E - E\Psi)^\mathsf{T}
\end{aligned}$$

and $\hat{\eta}_k$ and P_k° are the moments of the current navigation probability density, that is, $p(\eta_k \,|\, y^k) = \mathcal{N}(\eta_k, \hat{\eta}_k, P_k^\circ)$.

Proof: From the definition of conditional probability and the total probability theorem, and by exploiting the dependencies and independencies visualized in Figure 1, we find that

$$\begin{aligned}
p(x_{k+1}^b \,|\, x_k^b) = \frac{1}{p(x_k^b)} \int & p(x_{k+1}^b \,|\, x_{k+1}^w, \eta_{k+1})\, p(x_{k+1}^w \,|\, x_k^w) \\
& p(x_k^w \,|\, x_k^b, \eta_k)\, p(\eta_{k+1} \,|\, \eta_k) \\
& p(x_k^b, \eta_k)\, \mathrm{d}x_{k+1}^w\, \mathrm{d}x_k^w\, \mathrm{d}\eta_{k+1}\, \mathrm{d}\eta_k.
\end{aligned}$$

where all dependence on previous measurements have been suppressed for simpler notation. In the ingenuous body filter we make the assumption that $p(x_k^b, \eta_k) \approx p(x_k^b)\, p(\eta_k)$, which allows cancellation of the denominator. The densities involved in $p(x_{k+1}^b \,|\, x_k^b)$ can be written as

$$\begin{aligned}
p(x_k^w \,|\, x_k^b, \eta_k) &= \delta(x_k^w - x_k^b - E\eta_k) \\
p(x_{k+1}^b \,|\, x_{k+1}^w, \eta_{k+1}) &= \delta(x_{k+1}^w - x_{k+1}^b - E\eta_{k+1}) \\
p(\eta_k) &= \mathcal{N}(\eta_k \,;\, \hat{\eta}_k, P_k^\circ) \\
p(x_{k+1}^w \,|\, x_k^w) &= \mathcal{N}\left(x_{k+1}^w \,;\, \Phi\hat{x}_k^w, Q\right) \\
p(\eta_{k+1} \,|\, \eta_k) &= \mathcal{N}\left(\eta_{k+1} \,;\, \Psi\eta_k + u_{k+1}, Q^\circ\right).
\end{aligned}$$

By stacking all the Gaussians together in one joint Gaussian, and integrating over x^w_{k+1} and x^w_k, we get

$$p(x^b_{k+1} \,|\, x^b_k) = \int \mathcal{N}\left(\begin{bmatrix} x^b_{k+1} + E\eta_{k+1} \\ \eta_{k+1} \\ \eta_k \end{bmatrix}; \begin{bmatrix} \Phi(x^b_k + E\eta_k) \\ \Psi\eta_k + u_{k+1} \\ \hat{\eta}_k \end{bmatrix}, \begin{bmatrix} Q & 0 & 0 \\ 0 & Q^\circ & 0 \\ 0 & 0 & P^\circ_k \end{bmatrix} \right) \mathrm{d}\eta_{k+1}\, \mathrm{d}\eta_k$$

In order to marginalize away η_{k+1} and η_k we need to transform this into a Gaussian where x^b_{k+1}, η_{k+1} and η_k only enter as a stacked vector in the random vector slot (and not in the expectation slot). For this purpose we define the vectors

$$\beta = \begin{bmatrix} x^b_{k+1} \\ \eta_{k+1} \\ \eta_k \end{bmatrix}, \quad \zeta = \begin{bmatrix} \Phi x^b_k \\ u_{k+1} \\ \hat{\eta}_k + u_{k+1} \end{bmatrix}$$

and the matrices

$$A = \begin{bmatrix} I & E & -\Phi E \\ 0 & I & -\Psi \\ 0 & 0 & I \end{bmatrix}, \quad \tilde{Q} = \begin{bmatrix} Q & 0 & 0 \\ 0 & Q^\circ & 0 \\ 0 & 0 & P^\circ_k \end{bmatrix}.$$

With these notations, the expression for $p(x^b_{k+1} \,|\, x^b_k)$ becomes

$$\begin{aligned} p(x^b_{k+1} \,|\, x^b_k) &= \int \mathcal{N}\left(A\beta;\, \zeta,\, \tilde{Q}\right) \mathrm{d}\eta_{k+1}\, \mathrm{d}\eta_k \\ &= \int \mathcal{N}\left(\beta;\, A^{-1}\zeta,\, A^{-1}\tilde{Q}(A^{-1})^\mathsf{T}\right) \mathrm{d}\eta_{k+1}\, \mathrm{d}\eta_k. \end{aligned}$$

Inverting A is straightforward by means of standard results for block matrices. The proposition follows from picking the upper 2×1-vector in $A^{-1}\zeta$ and the upper left 2×2-matrix in $A^{-1}\tilde{Q}(A^{-1})^\mathsf{T}$. ■

The ownship update and absence of reframing— When an ownship measurement y_k is received, the ownship state is updated according to the standard Kalman filter correction step using the model described in Section 3. For the same reason as in the pure world filter, nothing happens to the target estimate during this step.

The target update—For the ingenuous body filter, the target state x^b_k is updated by means of a standard Kalman filter correction step with the measurement model $p(z_k \,|\, x^b_k) = \mathcal{N}(z_k\,;\, Hx^b_k, R)$. In this step, again due to the assumed independence, nothing happens with the ownship estimate.

The factitious body filter

The factitious body filter is very similar to the ingenuous body filter, but for this filter the velocity is parameterized in the world frame. Thus, its state vector is $x^f_k = \left[\rho^b_k, v^w_k\right]^\mathsf{T}$.

The propagation step— It can be shown in a manner very similar to the proof of Proposition 2 that

$$p(x^f_{k+1} \,|\, x^f_k) = \mathcal{N}(x^f_{k+1}\,;\, a^f_{k+1},\, Q^f_{k+1})$$

where

$$\begin{aligned} a^f_{k+1} &= \Phi x^f_k + (\Phi T - T\Psi)\,\hat{\eta}_k + Tu_{k+1} \\ Q^f_{k+1} &= Q + TQ^\circ T^\mathsf{T} + (\Phi T - T\Psi)\,P^\circ_k\,(\Phi T - T\Psi)^\mathsf{T}. \end{aligned}$$

The ownship update and absence of reframing— For the factitious body filter, the assumed independence between the target state and the ownship state again implies that the ownship update is carried out without affecting the target state estimate.

The target update—Again, the target state is updated using a likelihood of the form $p(z_k \,|\, x^f_k) = \mathcal{N}(z_k\,;\, Hx^f_k, R)$ without affecting the ownship state.

5. SIMULATIONS OF PURE FILTERING

Performance measures

For each filter and scenario we conduct 4000 Monte-Carlo simulations in order to study root mean square error (RMSE) and consistency. We study RMSE and covariance consistency separately for world frame position, body frame position, world frame velocity and body frame velocity.

For example, for the SLAM-like filter, which has the estimated state vector $\hat{\xi}_k = [\hat{\rho}^w_k, \hat{v}^w_k, \hat{\eta}^\mathsf{T}_k]^\mathsf{T}$ with the target state parameterized in the world frame, the raw and normalized world-frame errors are

$$\begin{aligned} e^w_{\mathrm{pos,k}} &= \rho^w_{k,\mathrm{true}} - \hat{\rho}^w_k \\ e^w_{\mathrm{vel,k}} &= v^w_{k,\mathrm{true}} - \hat{v}^w_k \\ c^w_{\mathrm{pos,k}} &= (\rho^w_{k,\mathrm{true}} - \hat{\rho}^w_k)^2 / P_{k,[11]} \\ c^w_{\mathrm{vel,k}} &= (v^w_{k,\mathrm{true}} - \hat{v}^w_k)^2 / P_{k,[22]} \end{aligned}$$

where $P_{k,[ij]}$ is the element in row number i and column number j in the covariance matrix provided by the filter. We use the root mean square normalized errors as a measure of consistency. For a good filter, these values should be close to one.

The body-frame estimates of target position and velocities are linear transformations of $\hat{\xi}_k$, given by $\hat{\rho}^b_k = [1, 0, -1, 0, 0]\hat{\xi}_k$ and $\hat{v}^b_k = [0, 1, 0, -1, 0]\hat{\xi}_k$ in the SLAM-like filter. Their corresponding covariances are given by

$$P^b_{k,\mathrm{pos}} = [1, 0, -1, 0, 0]P_k[1, 0, -1, 0, 0]^\mathsf{T} \tag{4}$$

$$P^b_{k,\mathrm{vel}} = [0, 1, 0, -1, 0]P_k[0, 1, 0, -1, 0]^\mathsf{T}. \tag{5}$$

The raw and normalized body-frame errors are

$$\begin{aligned} e^b_{\mathrm{pos,k}} &= \rho^b_{k,\mathrm{true}} - \hat{\rho}^b_k \\ e^b_{\mathrm{vel,k}} &= v^b_{k,\mathrm{true}} - \hat{v}^b_k \\ c^b_{\mathrm{pos,k}} &= (\rho^b_{k,\mathrm{true}} - \hat{\rho}^b_k)^2 / P^b_{k,\mathrm{pos}} \\ c^b_{\mathrm{vel,k}} &= (v^b_{k,\mathrm{true}} - \hat{v}^b_k)^2 / P^b_{k,\mathrm{vel}}. \end{aligned}$$

It is straightforward to evaluate these performance measures in the same way for the SKF's, since these filters also maintain a joint covariance matrix for the target state and ownship state.

For the correlation-free world filter, the raw and normalized errors in world frame are readily available. Also for this filter, we can construct a joint state estimate $\hat{\xi}_{k,\mathrm{world}} = [\hat{\rho}^w_k, \hat{v}^w_k, \hat{\eta}^\mathsf{T}_k]^\mathsf{T}$ where $\hat{\eta}_k$ in this case comes from

Quantity	Symbol/Units	High noise	Low noise
Ownship acceleration plant noise	σ_o^2 $[\mathrm{m}^2/\mathrm{s}^5]$	$(0.01)^2$	$(0.01)^2$
Bias time constant	$1/p$ [s]	1000	1000
Mean square bias	σ_b^2 $[\mathrm{m}/\mathrm{s}^2]$	$(0.1)^2$	$(0.1)^2$
GPS measurement noise	R_η $[\mathrm{m}^2]$	10^2	10^2
Accelerometer white noise	σ_w^2 $[\mathrm{m}^2/\mathrm{s}^3]$	$(0.0002)^2$	$(0.0002)^2$
Target measurement noise	R $[\mathrm{m}^2]$	$(0.2)^2$	$(0.01)^2$
Target plant noise	σ_v^2 $[\mathrm{m}^2/\mathrm{s}^3]$	$(1.0)^2$	$(0.05)^2$
Acceleration sampling time	[s]	0.01	0.01
Target measurement sampling time	[s]	2.5	2.5
GPS sampling time	[s]	1.0	1.0

Table 1: Simulation parameters

the standalone ownship navigation filter. The body frame estimates are then available as linear transformations of $\hat{\xi}_{k,\mathrm{world}}$ according to $\hat{\rho}_k^b = [1,0,-1,0,0]\hat{\xi}_{k,\mathrm{world}}$ and $\hat{v}_k^b = [0,1,0,-1,0]\hat{\xi}_{k,\mathrm{world}}$. To get the normalized errors we construct a joint covariance matrix, which in this case becomes block-diagonal since no cross-correlations are maintained. The joint covariance is again transformed according to (5). We proceed in a similar manner for the correlation-free body filters and for the basic world filter.

Simulation setup

Two cars drive on a straight road over a time span of 100 seconds. The first car, hereafter referred to as ownship, begins at $0\,\mathrm{m}$ with velocity $10\ \mathrm{m/s}$, while the second car, hereafter referred to as target, begins at $800\,\mathrm{m}$ with velocity $10\,\mathrm{m/s}$. The ownship accelerates with up to $1.5\,\mathrm{m/s^2}$ in the time interval 5s-25s, and decelerates by up to $2.5\,\mathrm{m/s^2}$ in the time interval 50s-52s. The target then accelerates by $1.5\,\mathrm{m/s^2}$ during the time interval 80s-85s.

The scenario can be divided into three phases: In the *transient phase* (0s-50s), the ownship filter is still working on estimating its own accelerometer bias, and this has a noticeable impact on several of the tracking filters. In the *stationary phase* (50s-80s), the bias has been estimated. The deceleration of the ownship is less noticeable in the error statistics, since the bias now is under control. In the *mismatch phase* (50s-100s), the target accelerates more than what the process noise accounts for, and this has a huge impact on the error statistics.

The differences between the tracking filters are most pronounced when the process noise of the target is low. Therefore we run both a realistic *high noise* version of the scenario, and a more ideal *low noise* version of the scenario, with tuning parameters as given in Table 1.

Observations and discussion

Overall results from the Monte-Carlo simulations are displayed in Tables 2-13. Furthermore, curves for RMSE and consistency are shown for the body frame velocity in Figures 2 and 3, respectively. Results for the mismatch phases are excluded in the figures in order to improve the resolution for transient and stationary phases.

The impact of navigation uncertainty compensation in general—The basic world filter is substantially inferior to the other filters in several contexts. In the transient phase of the low noise case (Table 8) its normalized position error in the world frame is 177 times too large. In the same phase of the high noise case this is reduced to 6 times too large, which still is quite significant. Figure 2 reveals that its RMSE also can be quite bad for low noise. For high noise, this is much less pronounced.

The impact of noise levels—For the high-noise scenario, most of the filters have a comparable performance, although we see some tendencies with poor consistency for the factitious body filter (Table 2), and poor RMSE for the correlation-free world filter (Table 6), which should warrant some caution with these filters. In the low-noise case, these tendencies are increased (compare with Tables 8 and 12, respectively), and many more differences become visible. This is important, because it shows turning down the process noise (e.g., during debugging) can have unpredictable consequences for target tracking with navigation uncertainty.

RMSE of the corelation-free world filter—A cause for the poor body frame RMSE of the correlation-free world filter may be as follows: Since the target measurement noise is much lower than the GPS measurement noise, it is possible to estimate the body frame target position with higher accuracy than then navigation accuracy. The body-parameterized filters achieve this by working directly in body frame, while the SKFs and the SLAM-like filter achieve this by having access to relevant correlations. The correlation-free world filter is unable to utilize any of these benefits.

Body versus World parametrization—The body filters tend to have lower RMSE in the body frame, while the suboptimal world filters in many cases have lower RMSE in the world frame. For consistency, on the other hand, the picture is opposite: The *normalized* error decreases when we transform to the alternative frame. This happens for all the filters except the SLAM-like filter. The reason for this pattern is that both the SKFs and the correlation-free filters have an "excess" of ownship covariance, which inflates the covariance in the other frame through the transformations described in Section 5. For example, the target covariance and cross-covariance of the world SKF are quite similar to the corresponding quantities for the SLAM-like filter, while the ownship covariance used in the SKF is significantly higher than for the SLAM-like filter since the SKF does not exploit target measurements to improve the navigation.

Who has the best RMSE?—In the low-noise case, the body filters have significantly lower RMSE in the body frame, while their world frame RMSE values are not significantly worse than those of the suboptimal world filters. The ingenuous body filter has the best RMSE results of these, and is the only suboptimal filter that comes close to the SLAM-like filter

during the stationary phase of the low-noise scenario (Table 12). It is also worth noticing that the ingenuous body filter, and the other body filters to a lesser extent, outperform the SLAM-like filter with regard to world position error in the subsequent mismatch phase (Table 13).

Who has the best consistency?—All of the suboptimal filters exhibit significant inconsistency problems in the low-noise scenario. Nevertheless, every one of them also beats the consistency of the SLAM-like filter in one way or another during the mismatch phase. This provides an example of why one may want to avoid the optimal SLAM-like solution if model mismatch or similar issues are a concern.

For data association, consistency of the position estimates in the body frame is particularly important. During the mismatch phase, the world SKF achieves the lowest normalized error, and this filter also has impeccable concistency properties during the other two phases. In the low-noise scenario, this comes at the price of 3 to 25 times higher RMSE than for the SLAM-like filter, which may be well worth paying for the increased robustness.

Velocity inconsistency for the factitious body filter— The factitious body filter has the worst consistency properties of all the filters. For example in Table 9, this can be seen for both the world-frame and the body-frame velocities. We see in Figure 3 that this in particular is a problem during the transient phase. The cause of this has to do with the neglect of correlations between target velocity and ownship velocity in the factitious body filter. We outline the role of these correlations below:

From a handful of range measurements of the target, we can estimate its relative velocity v_k^b (assuming nearly constant ownship velocity), but to estimate its world-frame velocity v_k^w we must also have access to good navigation estimates. In the transient phase, when a good navigation solution still is under development, the poor estimability of the world-frame target velocity v_k^w translates into substantial cross-correlations between this quantity and the ownship velocity v_k°. During the prediction of the target state, it can be shown that these correlations should counteract growth in the correlations between ρ_k^b and v_k^w. However, as the correlations between v_k^w and v_k° are ignored in the factitious body filter, we end up with artificially high correlations between ρ_k^b and v_k^w. This again causes the target measurements to have too strong an impact on the covariance of v_k^w. This quantity is therefore artificially reduced, and this leads to inconsistency.

The quasi-commutators—The matrices $\Phi E - E\Psi$ and $\Phi T - T\Psi$ appear in the correlation-free body filters, and govern leakage of ownship uncertainty into the target process noise. These leakage terms are not of much significance for realistic values of the process noise. Nevertheless, for very low process noise, e.g., $\sigma_v = 10^{-4}\,\mathrm{m}^2/\mathrm{s}^3$, we have found that ignoring these terms will cause significant deterioration in position RMSE and consistency. Let us also remark that these matrices also arise in body-frame implementations of the SLAM-like filter, where they play a crucial role in propagating the cross-correlations discussed in the previous paragraph.

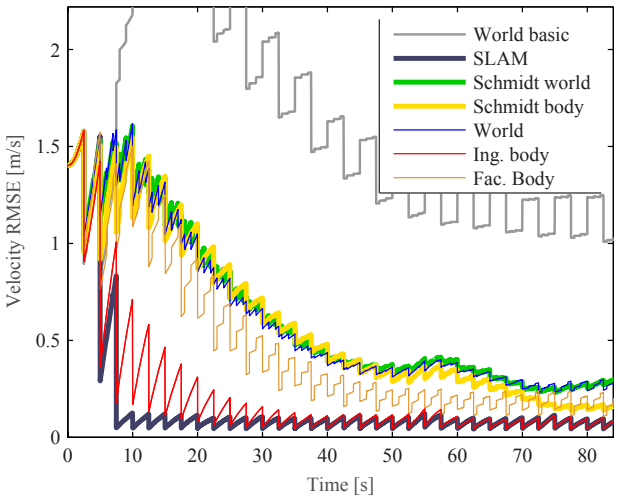

Figure 2: RMSE of target velocity decomposed in body frame for the low-noise scenario.

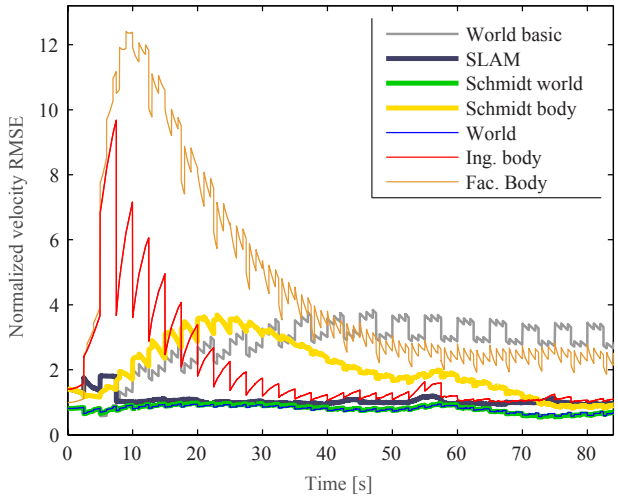

Figure 3: Consistency of target velocity decomposed in body frame for the low-noise scenario.

Table 2: Consistency: High noise, transient phase

	Pos. Body	Pos. World	Vel. Body	Vel. World
World basic	0.78	9.00	1.30	1.89
SLAM-like	1.06	0.99	1.03	0.99
Ingenuous Body	1.08	0.97	1.04	0.96
Factitious Body	1.13	0.98	1.11	1.25
World	0.57	1.09	0.87	0.97
Schmidt Body	1.05	0.96	1.03	0.94
Schmidt World	0.34	0.98	0.82	0.99

Table 3: Consistency: High noise, stationary phase

	Pos. Body	Pos. World	Vel. Body	Vel. World
World basic	0.64	6.95	1.30	1.38
SLAM-like	1.00	0.99	1.00	0.99
Ingenuous Body	1.00	0.99	1.00	0.99
Factitious Body	1.01	0.99	1.01	1.04
World	0.51	1.05	0.91	0.94
Schmidt Body	1.01	0.99	0.98	0.97
Schmidt World	0.28	0.99	0.94	1.00

Table 4: Consistency: High noise, target accelerates

	Pos. Body	Pos. World	Vel. Body	Vel. World
World basic	0.79	6.48	1.81	1.82
SLAM-like	1.46	1.01	1.62	1.51
Ingenuous Body	1.47	1.00	1.63	1.51
Factitious Body	1.47	1.00	1.63	1.55
World	0.71	1.13	1.55	1.52
Schmidt Body	1.48	1.01	1.61	1.49
Schmidt World	0.47	1.01	1.54	1.52

Table 5: RMSE: High noise, transient phase

	Pos. Body m	Pos. World m	Vel. Body m/s	Vel. World m/s
World basic	2.92	4.87	2.45	2.54
SLAM-like	1.88	5.21	1.48	1.61
Ingenuous Body	1.88	5.32	1.48	1.63
Factitious Body	2.02	5.37	1.60	1.73
World	4.63	6.42	1.98	1.98
Schmidt Body	2.06	5.32	1.63	1.72
Schmidt World	2.36	5.28	1.57	1.66

Table 6: RMSE: High noise, stationary phase

	Pos. Body m	Pos. World m	Vel. Body m/s	Vel. World m/s
World basic	2.91	4.87	1.85	1.88
SLAM-like	1.71	4.25	1.41	1.45
Ingenuous Body	1.71	4.26	1.41	1.45
Factitious Body	1.72	4.27	1.42	1.46
World	3.44	5.16	1.81	1.84
Schmidt Body	1.72	4.27	1.42	1.46
Schmidt World	1.72	4.26	1.42	1.45

Table 7: RMSE: High noise, target accelerates

	Pos. Body m	Pos. World m	Vel. Body m/s	Vel. World m/s
World basic	2.80	6.70	2.69	2.62
SLAM-like	2.78	4.35	2.40	2.30
Ingenuous Body	2.78	4.34	2.40	2.30
Factitious Body	2.78	4.33	2.40	2.29
World	4.88	5.79	3.13	3.03
Schmidt Body	2.80	4.37	2.43	2.32
Schmidt World	2.81	4.35	2.41	2.30

Table 8: Consistency: Low noise, transient phase

	Pos. Body	Pos. World	Vel. Body	Vel. World
World basic	0.62	177.28	3.19	31.67
SLAM-like	1.14	0.98	1.11	0.96
Ingenuous Body	2.98	0.96	3.12	0.84
Factitious Body	4.10	0.96	6.81	9.00
World	0.71	1.49	0.83	1.13
Schmidt Body	0.91	0.90	2.60	0.85
Schmidt World	0.61	0.94	0.86	0.92

Table 9: Consistency: Low noise, stationary phase

	Pos. Body	Pos. World	Vel. Body	Vel. World
World basic	0.60	137.66	3.19	19.15
SLAM-like	1.00	1.01	1.11	0.96
Ingenuous Body	1.11	0.99	3.21	0.84
Factitious Body	1.99	0.99	6.81	9.00
World	0.68	1.80	0.83	1.14
Schmidt Body	0.72	0.96	2.60	0.85
Schmidt World	0.50	1.01	0.86	0.92

Table 10: Consistency: Low noise, target accelerates

	Pos. Body	Pos. World	Vel. Body	Vel. World
World basic	0.82	128.03	6.16	30.51
SLAM-like	18.21	2.48	21.53	12.18
Ingenuous Body	21.68	1.02	25.89	4.87
Factitious Body	19.24	1.03	25.86	24.00
World	1.37	2.73	7.11	14.17
Schmidt Body	6.17	1.18	15.53	6.52
Schmidt World	1.23	1.97	7.10	12.95

Table 11: RMSE: Low noise, transient phase

	Pos. Body m	Pos. World m	Vel. Body m/s	Vel. World m/s
World basic	4.15	6.46	1.99	2.09
SLAM-like	0.78	3.74	0.46	0.45
Ingenuous Body	0.81	5.02	0.49	0.81
Factitious Body	1.15	5.00	0.81	0.92
World	4.39	4.82	0.93	0.46
Schmidt Body	1.31	4.84	0.92	0.83
Schmidt World	3.87	3.61	0.94	0.42

Table 12: RMSE: Low noise, stationary phase

	Pos. Body m	Pos. World m	Vel. Body m/s	Vel. World m/s
World basic	2.38	4.58	1.99	2.09
SLAM-like	0.09	3.14	0.08	0.21
Ingenuous Body	0.10	3.91	0.08	0.32
Factitious Body	0.23	3.91	0.19	0.35
World	3.07	4.01	0.31	0.25
Schmidt Body	0.36	3.84	0.26	0.32
Schmidt World	2.54	3.19	0.32	0.22

Table 13: RMSE: Low noise, target accelerates

	Pos. Body m	Pos. World m	Vel. Body m/s	Vel. World m/s
World basic	3.47	6.46	2.30	2.20
SLAM-like	2.00	7.75	1.79	2.57
Ingenuous Body	2.21	3.98	1.95	1.82
Factitious Body	2.38	4.05	2.07	1.93
World	6.19	6.10	2.96	2.81
Schmidt Body	3.47	4.68	2.80	2.66
Schmidt World	6.24	6.25	3.04	2.89

6. IMPACT ON DATA ASSOCIATION

One reason to investigate different parameterizations of moving platform target tracking is that the choices may affect susceptibility to clutter and misdetections. It was found in [13] that even small inaccuracies in navigation, due to EKF linearization, could seriously jeopardize data association for Bayesian SLAM. There exist dozens of different multi-target tracking algorithms that address data association, and a systematic study of how different multi-target tracking algorithms cope with navigation uncertainty is beyond the scope of this paper. Here we restrict attention to multi-dimensional assignment (MDA) implemented by means of Lagrangian Relaxation as described in Deb's paper [14]. This method can be viewed as a version of track-oriented multiple hypothesis tracking (TO-MHT) which attempts to find the most probable data association hypothesis over a sliding window of previous measurement scans.

Implementation of MDA

A Matlab implementation of Deb's method, adapted to moving platform tracking, was programmed. While the reader is referred to [14] for the details of the method, we provide a cursorial description of the method and implementation here.

Lagrangian Relaxation solves the data association problem for L scans (together with a list of tracks, hereafter referred to as the zeroth scan, making the problem $L+1$-dimensional) through an iterative process conducted until convergence. Each iteration consist of a relaxation phase and an enforcement phase. In the relaxation phase, the best assignments for scans $L-1$, $L-2$, ..., 0 are found by minimizing costs of the possible assignments at scans L, $L-1$, ..., 1. These costs involve both negative track scores [15] and Lagrange multipliers (there is one Lagrange multiplier for each non-dummy measurement). In the enforcement phase, assignments between candidate tracks at scans $0, 1, \ldots, L-1$ and measurements at scan number $1, 2, \ldots, L$ are constructed by means of the Auction algorithm [16]. After each iteration, the Lagrange multipliers are updated by means of a subgradient method. Whenever a measurement has been contended, that measurement is made less popular by means of the Lagrange multipliers.

We use Lagrangian Relaxation purely as a sliding window track maintenance method. We do not initialize new tracks, and neither do we allow tracks to die. The implementation uses a track tree in which different descents correspond to different possible tracks for each target. We use L-scan pruning on the track tree. We also prune tracks whose cost is 6 times higher than the cost of assigning all measurements to false alarms.

The MDA method is relatively straightforward to implement for all the filters, except the SLAM-like filter. For all the other filters, the dimensionless track score function of [15] is straightforward to adapt to our problem. The logarithmic contributions from different measurements and tracks at a given can be organized in a cost matrix, and the total cost of a data association hypothesis can be found by summing together elements from these matrices according to the chosen assignment.

For the SLAM-like filtering architecture, this cannot be done, at least not without additional approximations. The reason is that the unknown ownship state will affect the likelihood the measurements. The posterior probability of a data association hypothesis is an integral over the ownship state, and its logarithm cannot be decomposed into a sum of contributions from individual tracks [13]. This makes the construction of a *track-oriented* MHT or a JPDA for the SLAM-like tracking problem difficult. For this reason we omit the SLAM-like filter from the multi-target investigations.

Test design for multi-target simulations

We simulate 4 targets with initial states

$$x_0^{(1)} = \begin{bmatrix} 100 \\ 22 \end{bmatrix}, \; x_0^{(2)} = \begin{bmatrix} 50 \\ 10 \end{bmatrix},$$
$$x_0^{(3)} = \begin{bmatrix} 0 \\ 16 \end{bmatrix}, \; x_0^{(4)} = \begin{bmatrix} 150 \\ 2 \end{bmatrix},$$

over the time span $0 - 100\,\mathrm{s}$. This time we do not include any acceleration phase. The targets' kinematics are solely given by the plant model (1). Again, we study both the low noise and the high noise scenarios with parameters given in Table 1. The ownship simulation and all the ownship parameters are as before. We also include misdetections ($\mathrm{P_D} = 0.8$) and false alarms. We draw false alarms according to a Poisson cardinality distribution with expectation $\bar{\phi} = 15$ and according to a uniform spatial density extending $1000\mathrm{m}$ behind and in front of the ownship.

We study three performance measures: Track-loss rates including track swaps, track-loss rates not including track swaps and the OSPA metric with cutoff distance $20\,\mathrm{m}$ [17]. We define a track lost (possibly swapped) when the track shares none of the non-dummy measurements with the corresponding true track. We define a track lost, with swapping ignored, when the track has less than half its non-dummy measurements in common with any of the true tracks over the sliding window of the MDA. Other definitions of track-loss are possible, see [18,19].

Table 14: Track loss for multi-target low noise scenario

	Including swaps	Without swaps
World basic	48.90%	15.80%
Ingenuous Body	15.10%	5.80%
Factitious Body	21.25%	8.15%
World	3.10%	2.00%
Schmidt Body	4.50%	2.25%
Schmidt World	3.65%	2.25%

Table 15: Track loss for multi-target high noise scenario

	Including swaps	Without swaps
World basic	32.62%	6.81%
Ingenuous Body	16.19%	4.81%
Factitious Body	17.25%	4.44%
World	21.81%	5.06%
Schmidt Body	16.94%	4.37%
Schmidt World	16.88%	4.19%

Results for multi-target simulations

For the low noise case, track loss statistics are shown in Table 14. We make the following observations:

First, we notice that compensation of navigation uncertainty can decrease the track-loss rate by about a factor 10. Second, the correlation-free world filter emerges as the winner, with the Schmidt filters second. The correlation-free body filters suffer from noticeably higher track-loss rates. Based on this, one could argue that consistency in body frame is more important than RMSE in the body frame, since the world filters tend to have good consistency properties in the body frame, while the body filters tend to have lower RMSE in the body frame.

These observations are reflected in the OSPA metric between true world frame target states and the corresponding world frame estimates, displayed in Figure 4. The OSPA results for the correlation-free world filter and the SKFs are indistinguishable, and dominated by navigation uncertainty, while the other correlation-free filters have worse performance. A SLAM-like multi-target filter could possibly push the OSPA metric further down by 25% (cf., Table 12).

Results for the high noise case are displayed in Table 15 and Figure 5. As one would expect from comparison of the low-noise and high-noise results in Section 5, the differences in track-loss rates and OSPA metric between the different filters become less significant as the noise levels increase. Again, the basic world filter stands out as clearly inferior to the other filters. A couple of more surprising results can, however, be noticed. First, in the high noise scenario, the body-parameterized filters appear to outperform the correlation-free world filter. Second, track-loss rates and OSPA metric are often significantly lower than in the low noise scenario.

This is yet another illustration that low noise levels can be problematic when non-linearities (e.g., due to data association) and other sources of model mismatch are present. An obvious solution is to inflate Q and R in the filter model, but this may or may not be suitable depending on the application and the intended use of the tracking system.

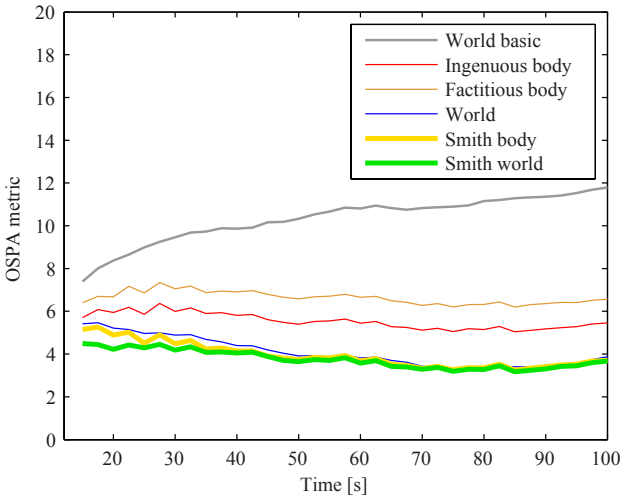

Figure 4: OSPA metric for the low noise case.

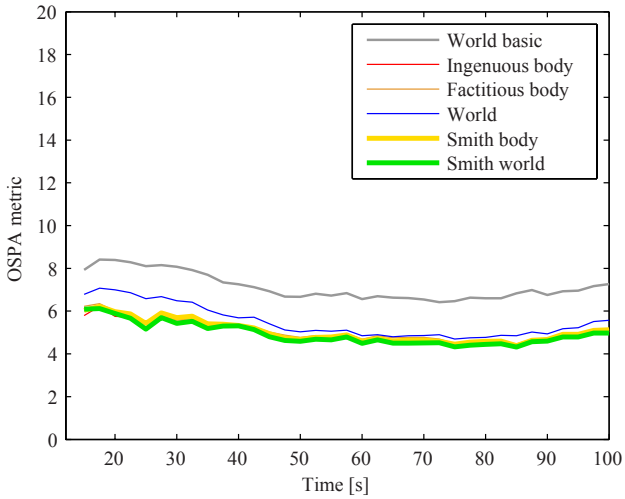

Figure 5: OSPA metric for the high noise case.

7. Conclusion and Future Research

Suboptimal filters such as Schmidt-Kalman filters or correlation-free filters with navigation uncertainty compensation may or may not achieve the same performance as the SLAM-like filter for target tracking on a moving platform. Body-parameterized filters appear preferable if body frame RMSE is important, while the world-parameterized Schmidt Kalman filter may be preferable from a consistency perspective. This filter also performs best when data association is involved. With basis in this paper and [3], where similar investigations were conducted in 6 degrees of freedom, future research may investigate the impact of various filtering architectures on data association in greater detail. The issues discussed in this paper are likely to be of increasing relevance the more SLAM-like a problem becomes. As an example in the aerospace setting, these issues are likely to be more relevant if one attempts to track a satellite from an airplane or a missile, than for the converse scenario.

ACKNOWLEDGMENTS

This work was supported by the Research Council of Norway through projects 223254 (Centre for Autonomous Marine Operations and Systems at NTNU) and 244116/O70 (Sensor Fusion and Collision Avoidance for Autonomous Marine Vehicles).

REFERENCES

[1] J. Solà, "Quaternion kinematics for the error-state KF," Mar. 2015. [Online]. Available: http://www.iri.upc.edu/people/jsola/JoanSola/objectes/notes/kinematics.pdf

[2] F. L. Markley, "Attitude error representations for kalman filtering," *Journal of Guidance, Control, and Dynamics*, vol. 26, no. 2, pp. 311 – 317, 2003.

[3] E. F. Wilthil and E. F. Brekke, "Compensation of navigation uncertainty for target tracking on a moving platform," in *Proceedings of Fusion 2016*, Heidelberg, Germany, Jul. 2016.

[4] C. S. Lee, D. E. Clark, and J. Salvi, "SLAM with dynamic targets via single-cluster PHD filtering," *IEEE Journal of Selected Topics in Signal Processing*, vol. 7, no. 3, pp. 543 – 552, Jun. 2013.

[5] E. Brekke, B. Kalyan, and M. Chitre, "A novel formulation of the Bayes recursion for single-cluster filtering," in *Proceedings of IEEE Aerospace Conference*, Big Sky, MT, USA, Mar. 2014.

[6] S. Julier and A. Gning, "Bernoulli filtering on a moving platform," in *Proceedings of Fusion 2015*, Washington, D.C., USA, July 2015, pp. 1511–1518.

[7] J. Solà, "Towards visual localization, mapping and moving objects tracking by a mobile robot: a geometric and probabilistic approach," Ph.D. dissertation, l'Institut National Politechnique de Toulouse, 2007.

[8] Y. Bar-Shalom, "Mobile radar bias estimation using unknown location targets," in *Proceedings of Fusion 2000*, Paris, France, 2000, pp. 3–6.

[9] R. Novoselov, S. Herman, S. Gadaleta, and A. Poore, "Mitigating the effects of residual biases with Schmidt-Kalman filtering," in *Proceedings of Fusion 2005*, Philadelphia, PA, USA, July 2005.

[10] C. Yang, E. Blasch, and P. Douville, "Design of Schmidt-Kalman filter for target tracking with navigation errors," in *Proceedings of IEEE Aerospace Conference*, Big Sky, MT, USA, Mar. 2010, pp. 1–12.

[11] C. Van Loan, "Computing integrals involving the matrix exponential," *IEEE Transactions on Automatic Control*, vol. 23, no. 3, pp. 395–404, 1978.

[12] M. Ulmke, O. Erdinc, and P. K. Willett, "Gaussian mixture cardinalized PHD filter for ground moving target tracking," in *Proceedings of Fusion 2007*, Quebec, Canada, July 2007.

[13] E. Brekke and M. Chitre, "A multi-hypothesis solution to data association for the two-frame SLAM problem," *The International Journal of Robotics Research*, vol. 34, no. 1, pp. 43–63, 2015.

[14] S. Deb, M. Yeddanapudi, K. Pattipati, and Y. Bar-Shalom, "A generalized S-D assignment algorithm for multisensor-multitarget state estimation," *IEEE Transactions on Aerospace and Electronic Systems*, vol. 33, no. 2, pp. 523–538, Apr. 1997.

[15] Y. Bar-Shalom, S. S. Blackman, and R. J. Fitzgerald, "Dimensionless score function for multiple hypothesis tracking," *IEEE Transactions on Aerospace and Electronic Systems*, vol. 43, no. 1, pp. 392–400, Jan. 2007.

[16] S. Blackman and R. Popoli, *Design and Analysis of Modern Tracking Systems*. Norwood, MA, USA: Artech House, 1999.

[17] D. Schuhmacher, B. T. Vo, and B.-N. Vo, "A consistent metric for performance evaluation of multi-object filters," *IEEE Transactions on Signal Processing*, vol. 56, pp. 3447–3457, Aug. 2008.

[18] S. Coraluppi, D. Grimmett, and P. D. Theije, "Benchmark evaluation of multistatic trackers," in *Proceedings of Fusion 2006*, Florence, Italy, July 2006.

[19] E. Brekke, O. Hallingstad, and J. Glattetre, "The Modified Riccati Equation for Amplitude-Aided Target Tracking in Heavy-Tailed Clutter," *IEEE Transactions on Aerospace and Electronic Systems*, vol. 47, no. 4, pp. 2874 – 2886, October 2011.

BIOGRAPHY

Edmund F. Brekke *has an MSc (2005) in Industrial Mathematics and a PhD (2010) in Engineering Cybernetics, both awarded by NTNU. His PhD research covered methods for target tracking using active sonar. This research was conducted at the University Graduate Center at Kjeller in collaboration with Kongsberg Maritime. After his PhD studies, Brekke worked as a postdoctoral research fellow at the Acoustic Research Lab at NUS in Singapore, before becoming an Associate Professor in Sensor Fusion at NTNU in 2014. Brekke's main research interests lie in Bayesian estimation, with applications in target tracking and autonomous navigation. Brekke is project manager of the competence-building reseach project "Sensor fusion and collision avoidance for autonomous surface vehicles" funded by the Research Council of Norway, Kongsberg Maritime, DNV GL and Maritime Robotics.*

Erik F. Wilthil *is a PhD candidate at the Department of Engineering Cybernetics at NTNU. He obtained his M.Sc. at the same department in 2015, and specialized in navigation systems for unmanned aerial vehicles. He is currently working on target tracking and navigation for the project "Sensor fusion and collision avoidance for autonomous surface vehicles".*